ORIGINAL PAPER

Trends in middle- and upper-level tropospheric humidity from NCEP reanalysis data

Garth Paltridge · Albert Arking · Michael Pook

Abstract The National Centers for Environmental Prediction (NCEP) reanalysis data on tropospheric humidity are examined for the period 1973 to 2007. It is accepted that radiosonde-derived humidity data must be treated with great caution, particularly at altitudes above the 500 hPa pressure level. With that caveat, the face-value 35-year trend in zonal-average annual-average specific humidity q is significantly negative at all altitudes above 850 hPa (roughly the top of the convective boundary layer) in the tropics and southern midlatitudes and at altitudes above 600 hPa in the northern midlatitudes. It is significantly positive below 850 hPa in all three zones, as might be expected in a mixed layer with rising temperatures over a moist surface. The results are qualitatively consistent with trends in NCEP atmospheric temperatures (which must also be treated with great caution) that show an increase in the stability of the convective boundary layer as the global temperature has risen over the period. The upper-level negative trends in q are inconsistent with climate-model calculations and are largely (but not completely) inconsistent with satellite data. Water vapor feedback in climate models is positive mainly because of their roughly constant

G. Paltridge (✉)
Environmental Biology Group, RSBS, Australian National
University,
GPO Box 475, Canberra, ACT 2601, Australia
e-mail: paltridge@iinet.net.au

A. Arking
Johns Hopkins University,
Baltimore, MD, USA

M. Pook
Centre for Australian Weather and Climate Research,
Hobart, TAS, Australia

relative humidity (i.e., increasing q) in the mid-to-upper troposphere as the planet warms. Negative trends in q as found in the NCEP data would imply that long-term water vapor feedback is negative—that it would reduce rather than amplify the response of the climate system to external forcing such as that from increasing atmospheric CO_2. In this context, it is important to establish what (if any) aspects of the observed trends survive detailed examination of the impact of past changes of radiosonde instrumentation and protocol within the various international networks.

1 Introduction

Balloon-borne radiosonde measurements are the basis of the NCEP reanalysis atmospheric humidity data that are available for the entire globe at each of the standard pressure heights from 1,000 to 300 hPa. The data are continuous from 1948 to the present. However, radiosonde humidity measurements are notoriously unreliable and are usually dismissed out-of-hand as being unsuitable for detecting trends of water vapor in the upper troposphere (e.g., Soden et al. 2005). This is unfortunate, since the feedback response of water vapor at these upper levels is an important factor controlling the degree of global warming from increasing atmospheric CO_2.

Elliott and Gaffen (1991) examined problems of radiosonde humidity measurements for climate studies. They decided that data before 1973 are indeed unusable without adjustments to take account of instrumental changes and deficiencies. Since 1973, the instrumental changes have had less obvious impacts, but there are still problems with reporting practices—particularly the reporting of data from higher levels where both temperature and humidity are very low. They suggested that "data above 500 hPa, with the

possible exception of the tropics, are not reliable enough to draw conclusions about upper-level humidity. Even 500 hPa data may be unreliable at high latitudes."

In this study, we report the trends in water vapor that emerge from the NCEP data for the 35-year period from 1973 to 2007. The analysis is restricted to latitudes between 50° S and 50° N and to altitudes at which the zonal-average specific humidity is greater than 0.5 g/kg. Thus, in the tropics (20° S to 20° N), data from all the NCEP pressure levels up to 300 hPa are included. In the midlatitudes (20° to 50° of each hemisphere), data from all levels up to 500 hPa are included, together with the summer season data from 400 hPa. The criterion with regard to specific humidity is equivalent to a restriction of the analysis to levels where the zonal-average temperature is greater than about −30°C in the tropics and −20°C in midlatitudes.

1.1 Data and analysis

Monthly averages of specific humidity q, relative humidity RH, and air temperature T are available directly from the NCEP Reanalysis Derived Data provided by the NOAA/OAR/ESRL Physical Sciences Division from its web site at http://www.cdc.noaa.gov; see also Kalnay et al. (1996). The data are reported with 2.5° latitude–longitude geographic resolution, and in the case of q and RH, are limited to the eight standard pressure levels ranging from 1,000 to 300 hPa. The reanalysis "data" are actually the output of a global weather forecasting model operated in a mode that continuously assimilates observed data from the worldwide network of meteorological observations. In the case of humidity, all the observed upper-air input data are from radiosondes, unlike the data on temperature which come as well from various satellites as they have come on line (Kistler et al. 2001). The model interpolates meteorologically coherent values of q, RH, and T into those grid boxes where there are no actual measurements. The problems associated with reanalysis data sets, in general, and with changing observing systems, in particular, are discussed by Bengtsson et al. (2004) among others.

In this study, the monthly average NCEP values of q, RH, and T were averaged over each of the tropical and midlatitude zones to give zonal averages at each pressure level that take into account the variation of grid square area with latitude. The 35-year trends of the zonal averages of q and RH, obtained as least square linear fits to time series of the annual averages over the period 1973 to 2007, are plotted as a function of pressure in Fig. 1.

It is likely from the Elliot and Gaffen discussion that instrumental and reporting errors in radiosonde humidity data would emerge first in the coldest and driest regions. In that context, it is worth comparing the two graphs of

monthly average specific humidity given in Fig. 2. Graph (a) concerns the 850-hPa level of the southern hemisphere, where it is warm enough and humid enough to imagine that the data might be reasonably acceptable "as is". The summer and winter trends in q are very similar—as indeed are the summer and winter trends at all midlatitude levels up to 500 hPa. Graph (b) concerns the 400-hPa level of the northern hemisphere. Here, the summer and winter trends are significantly different in that the winter trend is virtually zero. A possible reason might be that the very low humidity at that height and in that season is of the same order as the instrumental accuracy. Another might be that the winter monthly averages are more often affected by operational protocols that automatically set a measured q to zero if it is less than a certain value. Suffice it to say that, in Fig. 1 (and later in Figs. 3 and 4), the trends in 400 hPa summer-month midlatitude humidity are used as proxies for the trends of
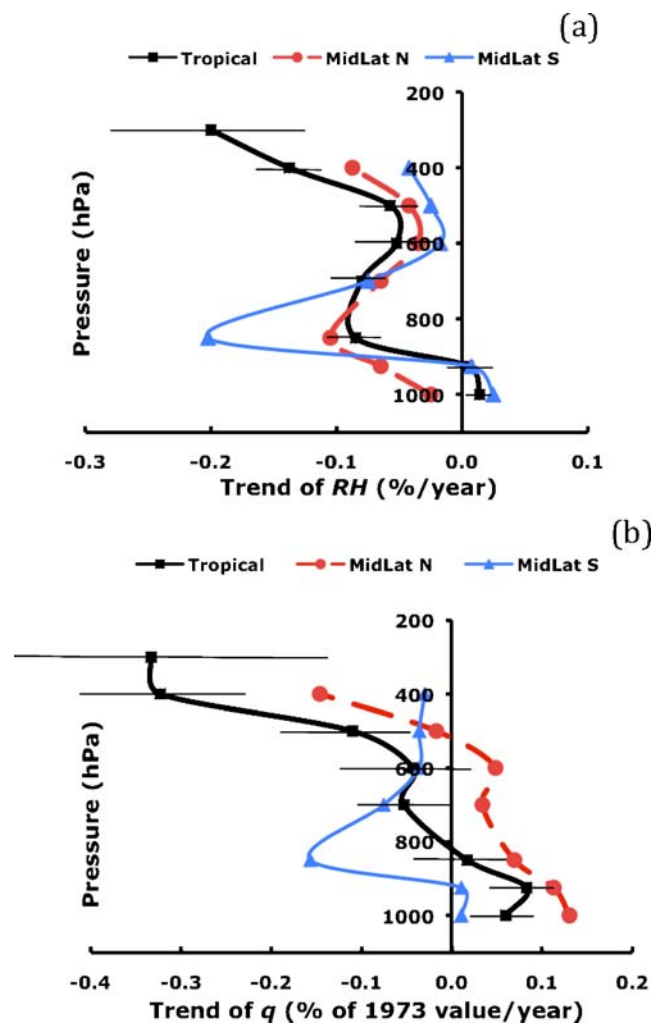

Fig. 1 Trends of average relative humidity RH (a) and specific humidity q (b) for three latitude zones, each as a function of pressure altitude. The range bars on the tropical profiles indicate the 95% confidence levels of the points on those profiles
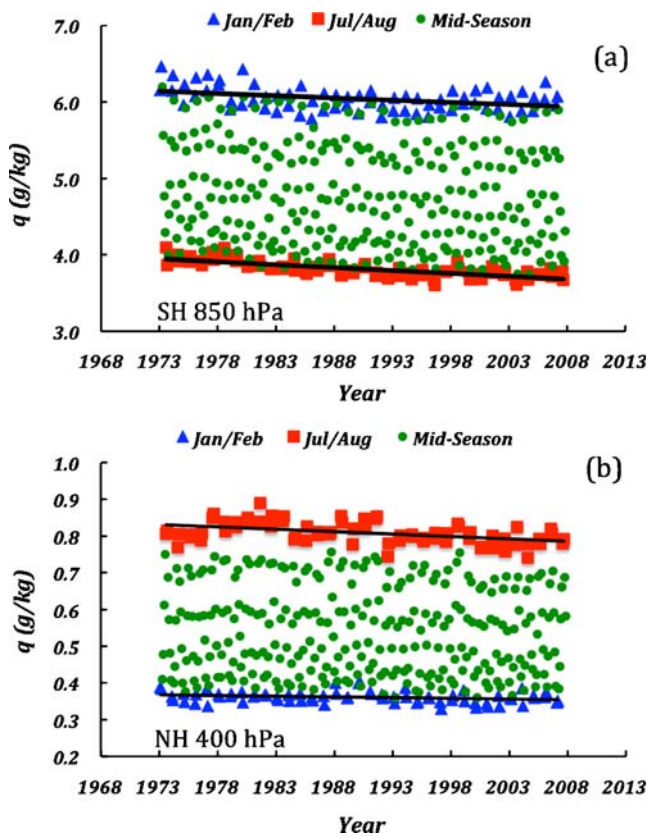
Fig. 2 a Southern hemisphere midlatitude monthly average specific humidity at 850 hPa as a function of time over the 35-year period 1973 to 2007. **b** Equivalent data for 400 hPa in the Northern hemisphere. The trend lines concern July/August data (*square red markers*) and January/February data (*triangular blue markers*). *Green dot markers* represent intermediate months

the annual averages at that height. The summer-month average q at 400 hPa (about 0.8 g/kg) is much the same as that of the winter-month average at 500 hPa.

The graphs of Figs. 3 and 4 are examples from each latitude zone of time series of the annual averages of q and RH. The central trend line in each case is a linear least square fit to the data. The slopes of the outer associated trend lines indicate the 95% confidence levels. They were calculated as described in Draper and Smith (1998) and refer only to the variability of the data and not to the potential error of the measurements. The range bars on the tropical trends in the two panels of Fig. 1 were inserted to illustrate the typical broad variation with height of the 95% confidence levels. The increase with height in the case of q is largely because the trends and confidence levels are displayed as the change per year expressed as a percentage of the 1973 value.

Upper-air data from a number of the radiosonde stations in tropical northern Australia were obtained from the Australian Bureau of Meteorology. The stations are part of the Global Climate Observing System (IGRA 2008) and provide input to

the NCEP reanalysis. Their record of monthly average specific humidity is essentially complete over the last 40-or-more years at all heights up to and including the 500-hPa level. However, the number of their "no data" months increases rapidly above that height, and there are generally not enough monthly averages at 300 hPa to perform any reasonable trend analysis. For this geographic region at least, but presumably also for much of the rest of the globe, the NCEP trend at 300 hPa (and to a lesser extent at 400 hPa) must be a model-generated reflection of the trend at the standard pressure level immediately below it.

The dry season (May through October) Australian tropical-station radiosonde data at 500 hPa show changes of a type that might be expected from, say, a change in the method of reporting very low values of humidity. The problem is not apparent in the wet season data where the absolute values of q are much greater, and it is the wet season data that largely determine the trends in the annual averages. The wet season (and annual-average) radiosonde data of the region show the same general profile of trends in q as the NCEP averages—namely, a switch from positive trends at the lowest altitudes to negative trends above the 850-hPa level.

Figure 5 is a repeat of the profile of the tropical specific humidity trends from Fig. 1, together with the profile obtained using NCEP data from only those tropical grid squares that have had continuous input since 1973 of observed data from the radiosondes of the Global Climate Observing System. There are 43 such grid squares, slightly less than 2% of the total tropical squares of the NCEP model. While there are some small differences between the profiles, the overall shapes are very similar. This is true also for each of the two midlatitude zones. The comparison suggests that the modeling and interpolation process of the NCEP calculations does not, of itself, introduce trends that differ significantly from the trends of the real observations. It also suggests that, as far as the zonal averages are concerned, the impact of any change in global radiosonde coverage since 1973 has been minimal.

Figure 5 also shows the profile of the tropical trends of q (averaged over all the NCEP tropical grid squares) for the first 35 years of the NCEP data set—that is, from 1948 to 1982. Despite the known problems with the radiosonde instrumentation before 1973 and despite a greater data variability, the overall profile of the trends is broadly similar to that of the most recent 35 years.

As an aside, although it bears slightly on the issue of data reliability, Figure 6 gives the geographic distribution of the trends of specific humidity at 400 hPa for the 34-year period 1973–2006. The colored areas are regions where the confidence levels of the trends are greater than 95%. White areas indicate a confidence less than 95% and effectively define regions where the trend is close to zero. There is a

Fig. 3 Examples of time series from 1973 to 2007 of annual-average specific humidity (in grams per kilogram) from each latitude zone and for three pressure levels. A linear trend line and two outer lines representing the associated 95% confidence levels are included on each example. Note that the data for the midlatitude 400-hPa level are actually summer season data (see text)
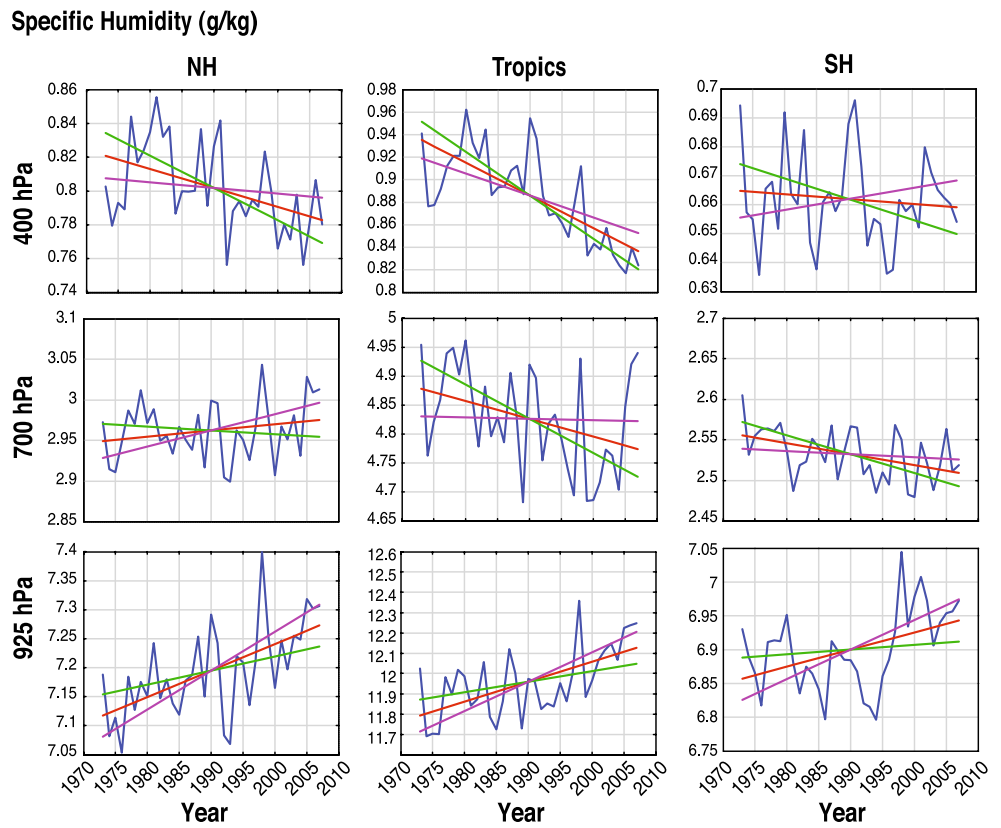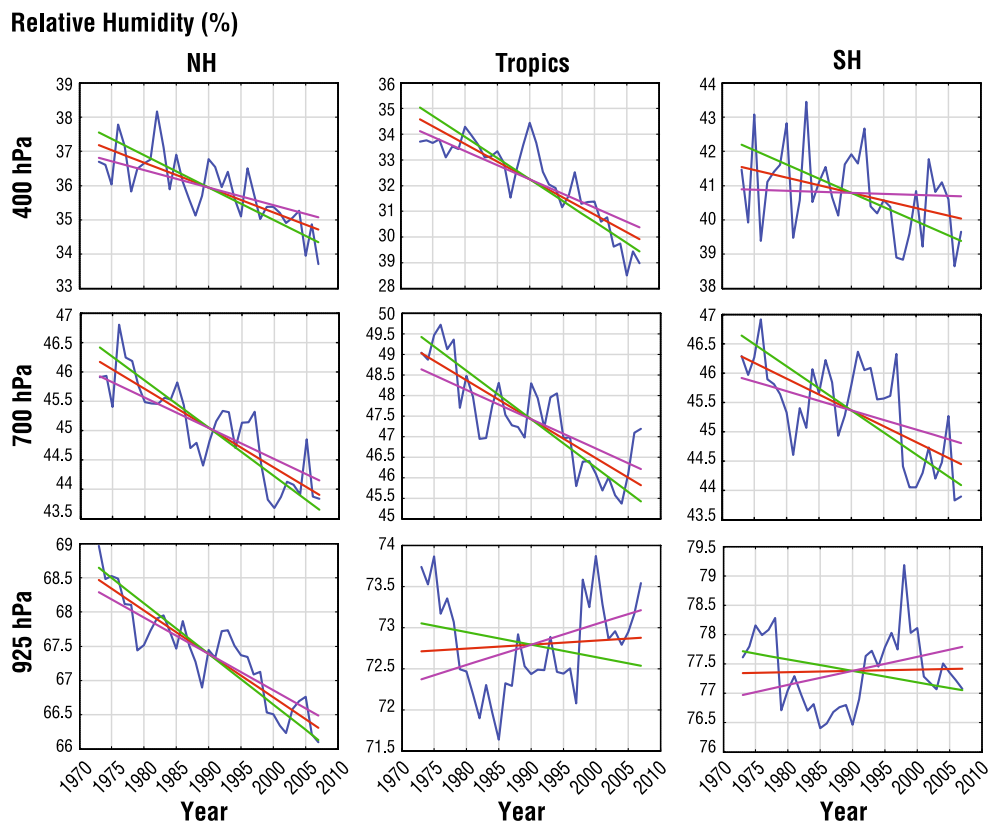

Specific Humidity (g/kg)

Fig. 4 Same as Fig. 3, but showing time series of annual-average relative humidity (in units of percent)
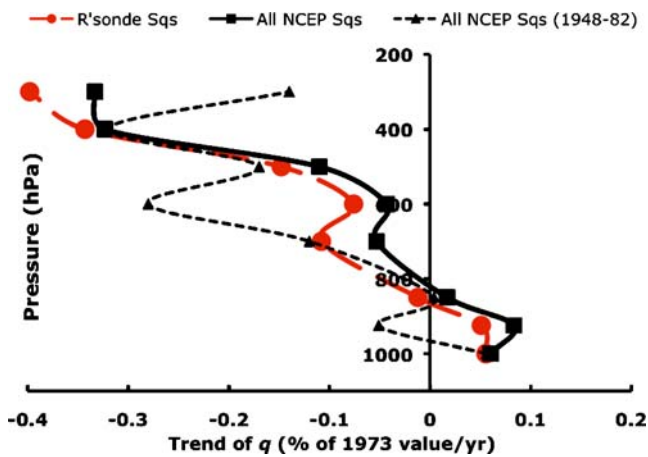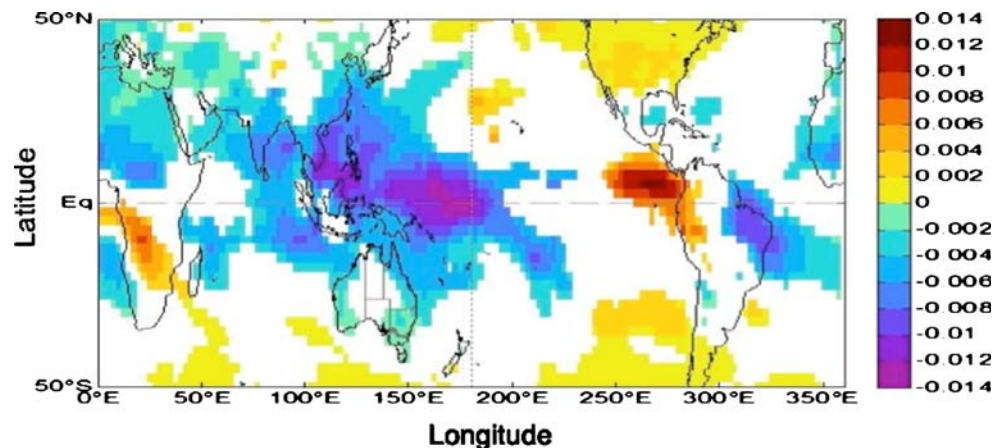

Relative Humidity (%)

Fig. 5 Comparison of the profile of the specific humidity trends obtained as an average of all NCEP tropical grid squares (the same as the tropical profile of Fig. 1b) and the profile obtained as an average only of those tropical squares in which there is an input of actual radiosonde data for the full 35-year period. Also shown is the profile obtained as an average of all tropical NCEP grid squares but for the period 1948 to 1982

significant positive trend over the tropical East Pacific and an extensive negative trend over the tropical areas to the north and north–east of Australia. It seems reasonable to imagine this pattern to be connected with the increase in the number of El Niño events over the last several decades (Guilderson and Schrag 1998; Trenberth and Hoar 1997). The connection would be via the similar pattern of change in observed sea surface temperature (and presumably also in the upward latent heat flux) associated with an increasing frequency of El Niño events. The assumption here is that some at least of the concentration of water vapor in the upper troposphere of a particular geographic region is determined by vertical turbulent diffusion of water vapor from the ocean surface immediately beneath.

Diagrams of the geographic distribution of the trends in specific humidity (similar in form to Fig. 6) were produced recently by Chen et al. (2008) for a number of pressure levels up to 400 hPa. Their diagrams compared

results from the NCEP and the European Centre for Medium-Range Weather Forecasting 40-year (ERA-40) reanalysis data sets. Unlike NCEP, the ERA-40 humidity information includes satellite data as they became available. The geographic spatial distributions from the two reanalyses are dissimilar at all the pressure levels. On the other hand, both reanalyses show a negative trend in the zonal averages of upper-level q.

2 Discussion

At face value then, the graphs of Figure 1 suggest the following.

First, the observations of relative humidity RH do not support the proposition that emerges from the behavior of general circulation climate models that the value of RH at any given height in the troposphere remains fairly constant under the influence of global warming (e.g., Soden and Held 2006; Pierrehumbert et al. 2007). The proposition is roughly supported by the data in the convective boundary layer, but at and above 850 hPa and for all three latitude zones, RH has decreased over the last three or four decades as the surface and atmospheric temperatures have increased. A particularly large decrease occurs at about 850 hPa in each of the latitude bands, presumably as a result of the maximum increase of temperature that occurs at that altitude. See later in discussion of Fig. 8. Another large decrease occurs above 500 hPa. Again, at face value, this decrease is a result of decreasing q as well as increasing T.

Second, while the specific humidity q has increased at the lowest levels of the troposphere over the last three or four decades in concert with the surface and 1,000 hPa temperatures, it has decreased in the middle and upper levels. This is particularly obvious in the tropics, where the crossover to negative trends occurs somewhere about 850 hPa—roughly near the top of the convective boundary layer. The crossover to negative values in the midlatitude

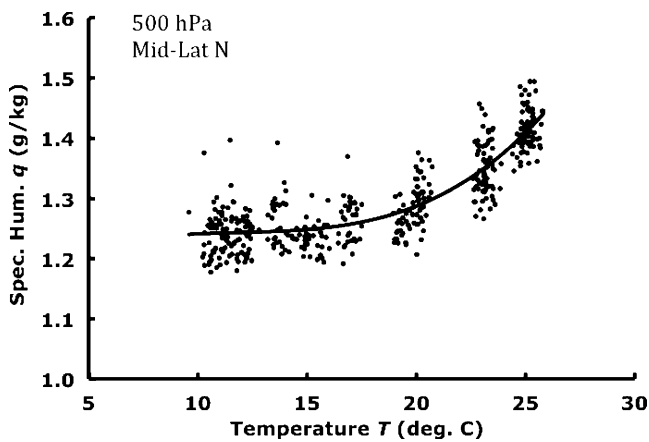**Fig. 6** Geographic distribution of the trend in annual-average specific humidity (in grams per kilogram per year) at 400 hPa over the period 1973 to 2006. *White regions* indicate areas where the confidence levels of the trends are less than 95%

Fig. 7 Northern midlatitude monthly average specific humidity q at 500 hPa for the full period 1973 to 2007 (the *dots*) plotted as a function of the corresponding monthly average air temperature at 1,000 hPa. The line is a least squares exponential fit

zones occurs at about 900 hPa in the southern hemisphere and at about 550 hPa in the northern hemisphere. These negative trends are not supported either by the predictions of climate models or by the few indications from satellite observations (e.g., Bates and Jackson 2001; Soden et al. 2005; Minschwaner and Dessler 2004) that the long-term trend of q in the upper troposphere is positive.

As with radiosonde measurements, satellite observations of upper-level humidity have their own problems and must be treated with caution. Most work to date concerns analysis of the channel 12 data of the High-Resolution Infrared Radiation Sounder (HIRS) of the NOAA polar orbiting satellites. Channel 12 is located near the center of the 6.7-μm rotational–vibrational emission band of water vapor and is sensitive both to the water vapor emission and to the temperature of a broad layer from about 200 to 500 hPa. Soden et al. (2005) find no trend in the global mean channel 12 radiance. Since model simulations with constant relative humidity also show no trend and simulations with constant specific humidity show a positive trend, they conclude that the HIRS observations are consistent with constant relative humidity. A potential practical issue concerns the fact that the positive trend for the constant q simulation appears only in the last 10 years of the 24-year simulation. Perhaps more to the present point, Bates and Jackson (2001) find wide variations in the HIRS-derived RH trend for different latitude zones. The trend is negative in the Southern Hemisphere between 10° and 60° S and negative in the Northern Hemisphere between 10° and 40° N. It is significantly positive only for the tropical zone from 10° N to 10° S.

The short-term correlation of NCEP upper-level humidity with surface temperature is strongly positive. Figure 7 is an example where the northern hemisphere midlatitude 500 hPa monthly average q is plotted as a simple function

of the corresponding 1,000 hPa T (effective surface temperature) for all months from 1973 to 2007. Such a positive correlation was reported from satellite measurements of seasonal differences nearly two decades ago (Rind et al. 1991). It is a consequence of the strong interaction between atmospheric levels via convection and vertical turbulent transfer. No doubt the relevant subgrid-scale representations of general circulation models are well-tuned to simulate this short-term interaction since the seasonal changes of q are large and because there are plentiful data, reliable in the short-term, with which to develop appropriate parameterization schemes.

It may be that the long-term trends in q (positive in the convective boundary layer and generally negative above it) can be explained in terms of the trends toward decreasing lapse rate within the convective boundary layer. Referring to Fig. 8, which shows the zonal-average trends in annual-average temperature according to the NCEP data, the temperature at 850 hPa has risen over the last few decades about 1/2 to 1°C more than at 1,000 hPa. This implies that the stability of the boundary layer has increased and, as a consequence, that the turbulent and convective transfer coefficients within it have decreased. In turn, this implies a tendency for the upward flux of water vapor through the top of the layer into the middle troposphere to be reduced. The question remains as to whether the tendency would be completely offset by an increasing water vapor (i.e., latent heat) flux from the surface—that is, by an increasing water vapor density in the boundary layer—or indeed as to whether the tendency
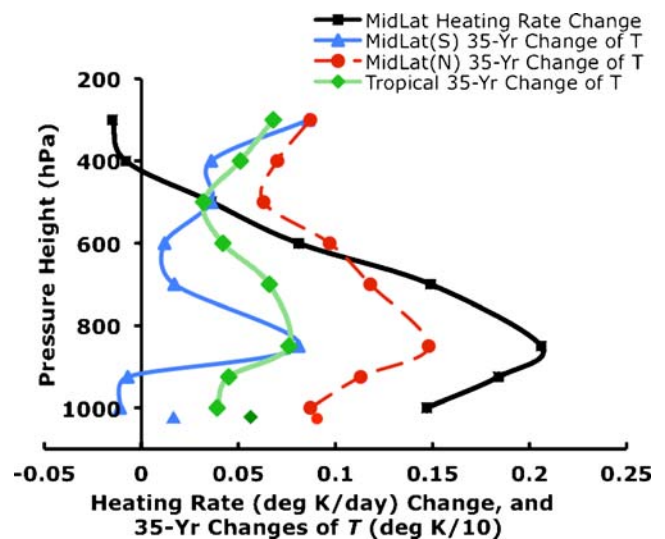

Fig. 8 The profiles of the trends from 1973 to 2007 of the annual average air temperature of each latitude zone according to the NCEP data. Also shown are the (1) profile of the change in midlatitude radiative heating rate that would occur with an instantaneous doubling of the concentration of atmospheric CO_2 and (2) markers at the 1,013 hPa level indicating the 35-year trend in surface temperature derived from the GHCN–ERSST data from NOAA (2008)

would be completely masked by water vapor large-scale transport from other geographical regions.

Furthermore, one must note the possible difficulties with NCEP temperature trends because (among other things) of changes in the observing system as satellite-derived temperatures were added to the radiosonde information as the data became available. As an example of the potential problems, Fig. 9 is time series plot of the "global average" (50° N to 50° S) temperature difference between the 800- and 1,000-hPa pressure levels. It shows an increase of the temperature difference in 1978 (also appearing in each of the individual latitude zones) of the order of 0.3°C. This is the year in which Television Infrared Observation Satellite sounder data were introduced into the NCEP reanalysis.

There are at least two possible reasons for the occurrence of a maximum in the long-term trend of temperature at (roughly) the 850-hPa level. First, the maximum increase in radiative heating of the atmosphere as a direct result of increasing CO_2 occurs at about that height. See, for example Figure 8, which includes the midlatitude profile of the increase in longwave radiative heating that would result from an instantaneous doubling of CO_2. Second, and perhaps more important in the present context, as the surface temperature rises because of increasing CO_2 (or indeed from any other cause), the upward flux of latent heat from the surface will (is expected to?) increase. This demands an increase of precipitation to balance the water budget of the atmosphere and, in turn, would ensure increased deposition of latent heat at those heights where there is a net conversion of water vapor into precipitation particles. In midlatitudes, the maximum rate of such conversion seems to occur somewhere near the freezing level. In tropical warm-rain situations, the maximum rate of
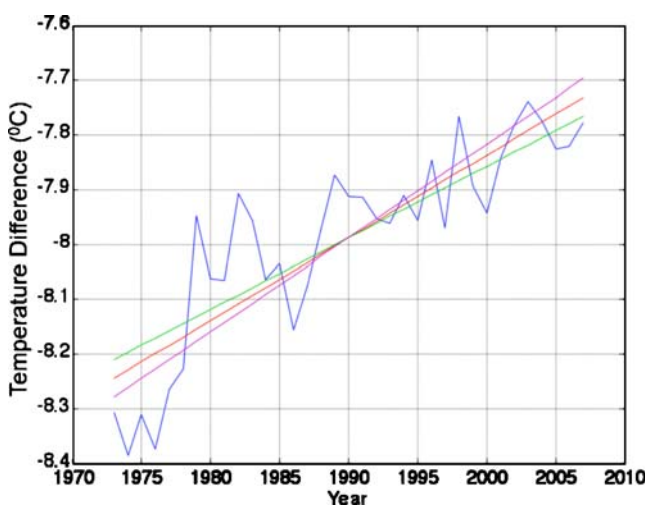
conversion occurs well below the freezing level. Either way, the height of maximum deposition of latent heat is presumably somewhere between 700 and 900 hPa.

3 Water vapor feedback

Water vapor feedback in climate models is large and positive (Bony et al. 2006). The various model representations and parameterizations of convection, turbulent transfer, and deposition of latent heat generally maintain a more-or-less constant relative humidity (i.e., an increasing specific humidity q) at all levels in the troposphere as the planet warms. The increasing q amplifies the response of surface temperature to increasing CO_2 by a factor of 2 or more.

Figure 10 illustrates the extent to which water vapor feedback is dependent on the constant relative humidity characteristic that is common to most climate models. It shows results from a one-dimensional radiative–convective equilibrium model designed specifically to bypass the detail of how convective processes respond to surface warming. The model is described in Arking (2005). The solar and terrestrial radiative fluxes at each level are computed using updated radiation routines based on the work of Chou and Arking (1980) and Chou et al. (1991). The model calculates an equilibrium temperature profile for a stratosphere in which the net radiative flux at each level is zero. Below the stratosphere is a convective layer identified with the troposphere, within which the temperature follows the moist adiabatic lapse rate. The height of this convective layer is determined by iteration—i.e., adjusted up or down —until the difference in temperature between the topmost layer of the troposphere and the first layer of the stratosphere is the smallest value that does not exceed the prescribed lapse rate. In all of the runs shown in the figure, the height of the convective layer turned out to be 220 hPa.

For the particular results of Fig. 10, the model was arranged so as to maintain a constant relative humidity within the planetary boundary layer (i.e., below the 800-hPa level) when the atmospheric concentration of CO_2 was doubled. Various prescribed profiles of specific humidity were imposed above the 800-hPa level as described in the caption. The fourth of these profiles is based on a simple average of the three zonal-average profiles of change of specific humidity shown in Fig. 1b. It is purely illustrative. It assumes an exponential rise of CO_2 concentration from its 1973 value into the future and a continuation of the linear trends in q up to the time when CO_2 has doubled—that is, in 2110 or thereabouts. It assumes the trends to be constant from 400 hPa up to the top level of the model at 100 hPa.

The figure shows that constant specific humidity in the upper troposphere effectively reduces to zero the water vapor

Fig. 9 The "global average" (50° N to 50° S) time series from 1973 to 2007 of the difference between the 850- and 1,000-hPa annual-average air temperatures according to the NCEP data, together with the linear trend and lines representing the 95% confidence levels
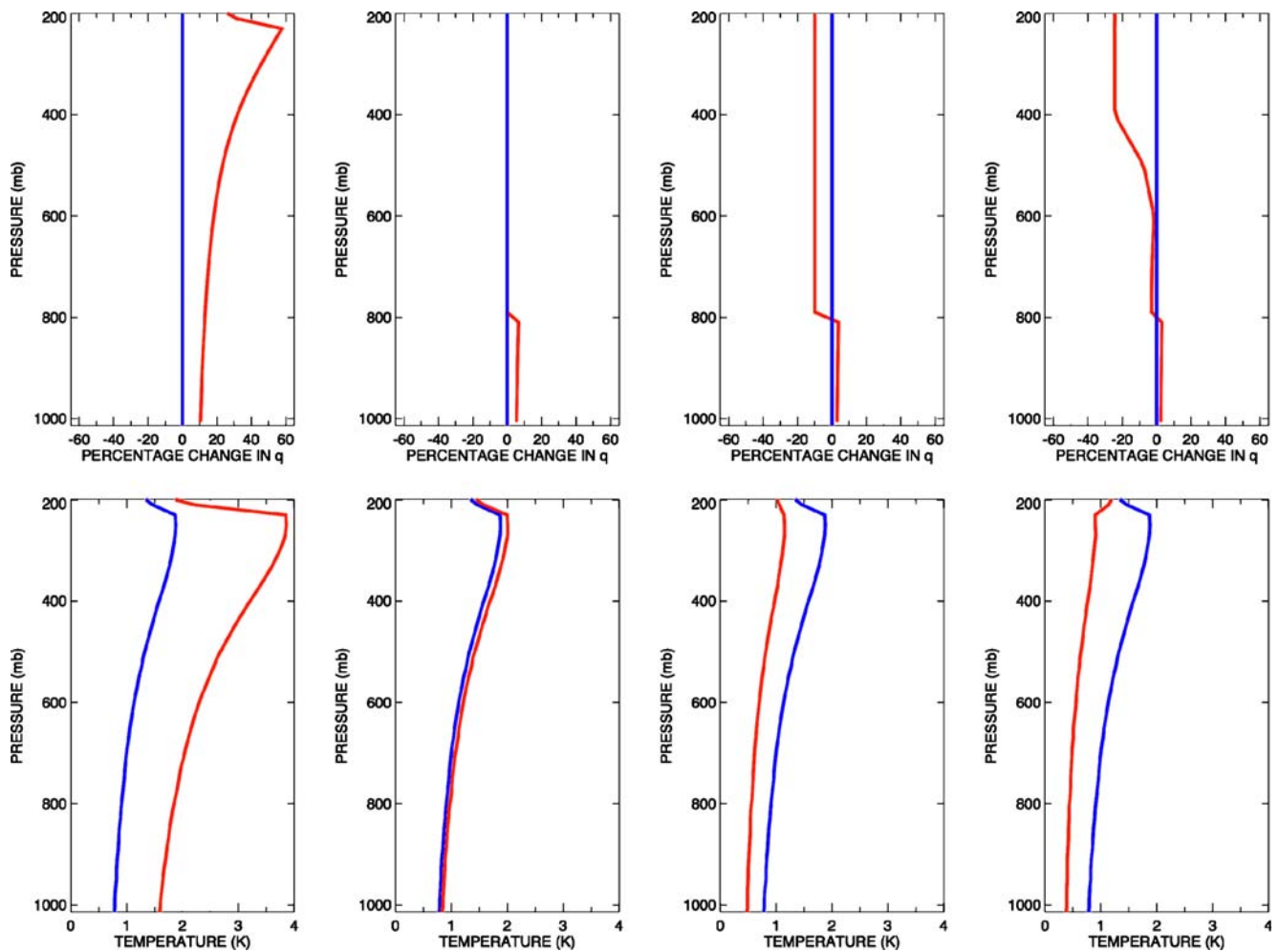
Fig. 10 The change in temperature from a doubling of CO_2 (*lower frames*) showing the effects of prescribed changes in the water vapor profile (*upper frames*) for a midlatitude summer standard atmosphere (McClatchey et al. 1972) without clouds and assuming a moist adiabatic lapse rate. Below the 800-hPa level, q is adjusted to keep the relative humidity fixed at the climatological value. Above the 800-hPa level, various changes in q are imposed: (from *left* to *right*) relative humidity fixed at the climatological value; no change; uniform decrease of 10%; and a profile based on the NCEP trends (see text). Each plot of temperature response shows the response with fixed humidity (*blue*) and with the prescribed change in humidity (*red*)

feedback in response to doubled CO_2. A decrease in mid-to-upper-level q produces negative feedback and a reduction of the CO_2-induced rise of surface and atmospheric temperature. Whatever the change in the upper levels, the overall water vapor in the total atmospheric column increases because changes in the large absolute values of q in the atmosphere below 800 hPa dominate the total. Put the other way around, increases in total column water vapor in response to global warming do not necessarily indicate positive water vapor feedback, since very small decreases of water vapor in the mid-to-upper troposphere can negate the effect of large increases in the boundary layer.

There have been discussions in the past (e.g., Lindzen 1990, Lindzen et al. 2001; Betts 1990; Spencer et al. 2007) about the theoretical possibility of a negative trend in upper-level humidity associated with global warming, and the issue has not been resolved. The many and various

mechanisms governing vertical transport of water vapor in the atmosphere include a number of subgrid-scale processes. Moist convection and turbulent diffusion for instance are among the most highly parameterized of all the simulated processes within an atmospheric model and are very difficult to verify. In particular (in view of the discussion earlier with reference to Fig. 7), it is not necessarily true that verification of the short-term simulation of vertical water vapor transport is sufficient for studies on the longer time scales of climate change.

4 Conclusion

It is of course possible that the observed humidity trends from the NCEP data are simply the result of problems with the instrumentation and operation of the global

radiosonde network from which the data are derived. The potential for such problems needs to be examined in detail in an effort rather similar to the effort now devoted to abstracting real surface temperature trends from the face-value data from individual stations of the international meteorological networks. As recommended by Elliot and Gaffen (1991) in their original study of the US radiosonde network, there needs to be a detailed examination of how radiosonde instrumentation, operating procedures, and recording practices of all nations have changed over the years and of how these changes may have impacted on the humidity data.

In the meantime, it is important that the trends of water vapor shown by the NCEP data for the middle and upper troposphere should not be "written off" simply on the basis that they are not supported by climate models—or indeed on the basis that they are not supported by the few relevant satellite measurements. There are still many problems associated with satellite retrieval of the humidity information pertaining to a particular level of the atmosphere—particularly in the upper troposphere. Basically, this is because an individual radiometric measurement is a complicated function not only of temperature and humidity (and perhaps of cloud cover because "cloud clearing" algorithms are not perfect), but is also a function of the vertical distribution of those variables over considerable depths of atmosphere. It is difficult to assign a trend in such measurements to an individual cause.

Since balloon data is the only alternative source of information on the past behavior of the middle and upper tropospheric humidity and since that behavior is the dominant control on water vapor feedback, it is important that as much information as possible be retrieved from within the "noise" of the potential errors.

References

Arking A (2005) Effects of bias in solar radiative transfer codes on global climate model simulations. Geophys Res Lett 32:L20717. doi:10.1029/2005GL023644

Bengtsson L, Hagemann S, Hodges KI (2004) Can climate trends be calculated from reanalysis data? J Geophys Res 109:D11111. doi:10.1029/2004JD004536

Betts AK (1990) Greenhouse warming and the tropical water budget. Bull Am Meteorol Soc 71:1464–1465

Bates JJ, Jackson DL (2001) Trends in upper-tropospheric humidity. Geophys Res Lett 28(9):1695–1698

Bony S et al (2006) How well do we understand and evaluate climate change feedback processes. J Climate 19:3445–3482

Chen J, DelGenio AD, Carlson BE, Bosilovich MG (2008) The spatiotemporal structure of twentieth-century climate variations in observations and reanalysis Part II: Pacific pan-decadal variability. J Climate 21:2634–2650

Chou MD, Arking A (1980) Computation of infrared cooling rates in water vapour bands. J Atmos Sci 37:855–867

Chou MD, Kratz DP, Ridgway W (1991) Infrared radiation parameterizations in numerical climate models. J Climate 4:424–437

Draper NR, Smith H (1998) Applied regression analysis, 3rd edn. Wiley Interscience, New York, p 706

Elliott WP, Gaffen DJ (1991) On the utility of radiosonde humidity archives for climate studies. Bull Am Meteorol Soc 72:1507–1519

Guilderson TP, Schrag DP (1998) Abrupt shift in subsurface temperatures in the tropical Pacific associated with changes in El Nino. Science 281(5374):240–243

IGRA (2008) Integrated Global Radiosonde Archive. See the 'igra-stations.txt' file available via http://www.ncdc.noaa.gov/oa/climate/igra/index.php

Kalnay E et al (1996) The NCEP/NCAR 40-year reanalysis project. Bull Am Meteorol Soc 77:437–470

Kistler R et al (2001) The NCEP-NCAR 50-year reanalysis: monthly means CD-ROM and documentation. Bull Am Meteorol Soc 82:247–267

Lindzen RS (1990) Some coolness concerning global warming. Bull Am Meteorol Soc 71:288–299

Lindzen RS, Ming-Dah C, Hou AY (2001) Does the earth have an adaptive iris? Bull Am Meteorol Soc 82:417–431

McClatchey RA, Fenn RW, Selby JEA, Volz FE, Garing JS (1972) Optical Properties of the Atmosphere, 3rd edn. Air Force Cambridge Research Laboratories, Report No. AFCRL-72-0497, L.G. Hanscom Field, Bedford MA

Minschwaner K, Dessler AE (2004) Water vapor feedback in the tropical upper troposphere: model results and observations. J Climate 5:5–21

NOAA (2008) Global climate at a glance. Available from National Climatic Data Center via http://www.ncdc.noaa.gov/gcag/gcag.html

Pierrehumbert RT, Brogniez H, Roca R (2007) On the relative humidity of the Earth's atmosphere. In: Schneider T, Sobel AH (eds) The global circulation of the atmosphere. Princeton University Press, Princeton, NJ, pp 143–185

Rind D, Chiou EW, Chu W, Larsen J, Oltmans SW, Lerner J, McCormick MP, McMaster L (1991) Positive water vapour feedback in climate models confirmed by satellite data. Nature 349:500–503

Soden BJ, Held IM (2006) An assessment of climate feedbacks in coupled ocean–atmosphere models. J Climate 19:3354–3360

Soden BJ, Jackson DL, Ramaswamy V, Schwarzkopf MD, Xianglei H (2005) The radiative signature of upper tropospheric moistening. Science 310:841–844

Spencer RW, Braswell WD, Christy JR, Hnilo J (2007) Cloud and radiation budget changes associated with tropical intraseasonal oscillations. Geophy Res Lett 34:L15707. doi:10.1029/2007GL029698

Trenberth KE, Hoar TJ (1997) El Nino and climate change. Geophys Res Lett 24(23):3057–3060